

Figure S1: Mn upregulates exosomal α Syn release. (A) Naïve MN9D cells were treated with $MnCl_2$ under serum-free conditions to establish an EC_{50} via MTT assay based on the average of three experiments performed in octuplicate. (B and C) Analysis of Western blotting for (B) GFP-fused α Syn and (C) LDHA in conditioned medium from MN9D cells over time. Data were analyzed using repeated measures three-way ANOVA with treatment (Mn effect), genotype, time and their interactions as fixed effects and sample as subject of repeated measurements. Data are mean \pm SEM (** $p < 0.01$, *** $p < 0.001$, ns = non-significant) of ≤ 6 experiments. (D) Western Blots (WBs) of exosome lysates (EL) and cell lysates (CL). The presence of canonical exosome proteins and the absence of Lamin and GRP78 demonstrate a pure EL preparation. (E) Concentration of exosomes from GFP_Syn cells, from vehicle-stimulated (red) and Mn-stimulated (blue) cells. (F) ELISA of exosomal α Syn concentrations. Data, normalized to vehicle-stimulated GFP_EV exosomes, are mean \pm SEM (** $p < 0.01$) of four experiments. (G) WBs of exosomes from MN9D cells transfected with either HA and 6X-His-tagged- α Syn or the control empty vector plasmid. (H) TEM of exosomes isolated through ExoQuickTC of exosomes secreted from α Syn_{HA/His} vector-transfected MN9D cells. (I and J) NanoSight particle tracking indicating sizes (I) and (J) concentration of exosomes from cells transfected with 6X-His-tagged- α Syn or the control empty vector plasmid. Data are mean \pm SEM (** $p < 0.01$) of four experiments. (K) Dot blot analysis of recombinant α Syn (r- α Syn) fibrils and monomers with exosome lysates indicating the specificity of α Syn-fibril specific antibody. (L) Thioflavin T-based α Syn RT-QuIC assay using aggregated recombinant α Syn as the “seed” and recombinant wild-type human α Syn as the “substrate”. Fluorescence intensity and the lag-phase directly correlate with the “seed” concentration.

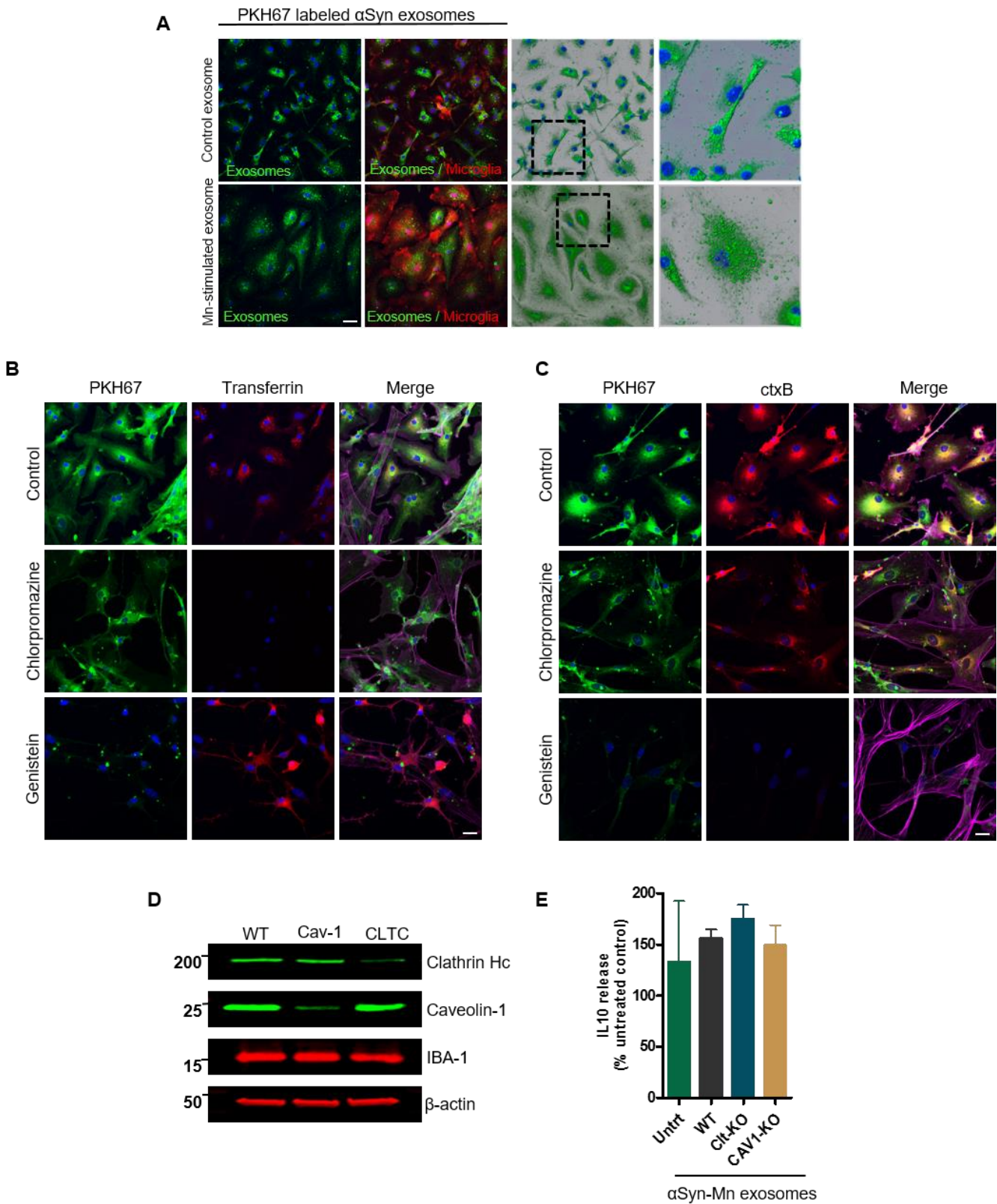


Figure S2: Exosomes internalize through caveolin-mediated endocytosis. (A) Confocal microscopy indicating homogeneous internalization of exosomes (PKH67; green) by microglial cells (IBA-1; red). Activated morphology was only observed upon internalization of Mn-stimulated (bottom panel), but not vehicle-stimulated (upper panel), α Syn-containing exosomes. The 3D surface reconstruction images generated by Imaris software (right two columns) show the differences in cellular morphology. Inset

shows (3X zoomed in) individual cell of original 60X image. **(B and C)** Primary microglial cells were exposed to Chlorpromazine and Genistein to inhibit clathrin-mediated and caveolae-mediated endocytosis, respectively, and co-treated with PKH67-labeled exosomes (green) and **(B)** Alexa-555-labeled transferrin (red) or **(C)** Alexa-555-labeled ctxB (red) to identify the primary facilitator for microglial internalization of neuronal exosomes. Immunofluorescence triple-labeling for exosomes (green), Alexa-555-labeled ctxB (red) and the cytoskeleton marker Alexa-647 phalloidin indicate that exosome internalization primarily occurred through caveolae-mediated endocytosis. **(D)** CRISPR/Cas9-mediated knockdown of caveolin-1 (CAV-1) and clathrin (CLTC) in primary murine microglial cells was confirmed with Western blotting. **(E)** IL-10 cytokine release upon exosome treatment was quantified using Luminex bead-based cytokine assays. Data are mean \pm SEM (** $p < 0.01$, *** $p < 0.001$) of four individual experiments performed in octuplicate.

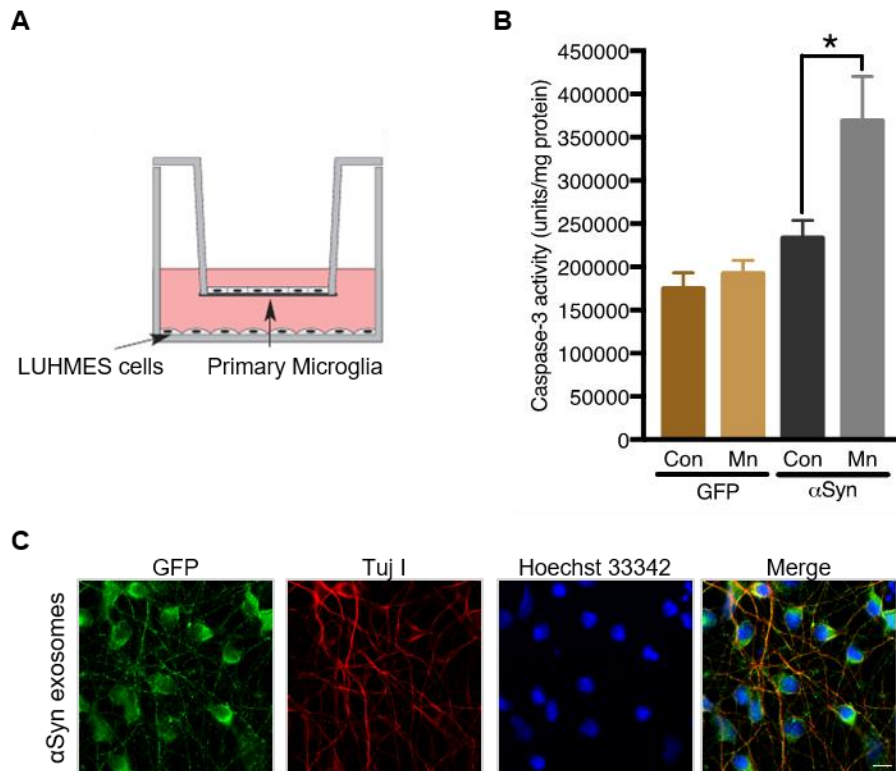


Figure S3: α Syn exosomes induce neuronal cell death *in vitro*. (A) Neuron-glia mixed culture system established using primary microglial cells and differentiated LUHMES cells. (B) Exosome-induced neuronal apoptosis measured by increased caspase-3 activity in differentiated LUHMES cells. Data are mean \pm SEM (* $p < 0.05$) of three individual experiments performed in duplicate. (C) Exosome uptake readily occurred in exosome-treated LUHMES cells as evidenced by GFP-immunoreactive (green) punctate structures inside the Tuj1-positive (red) neuronal cells.

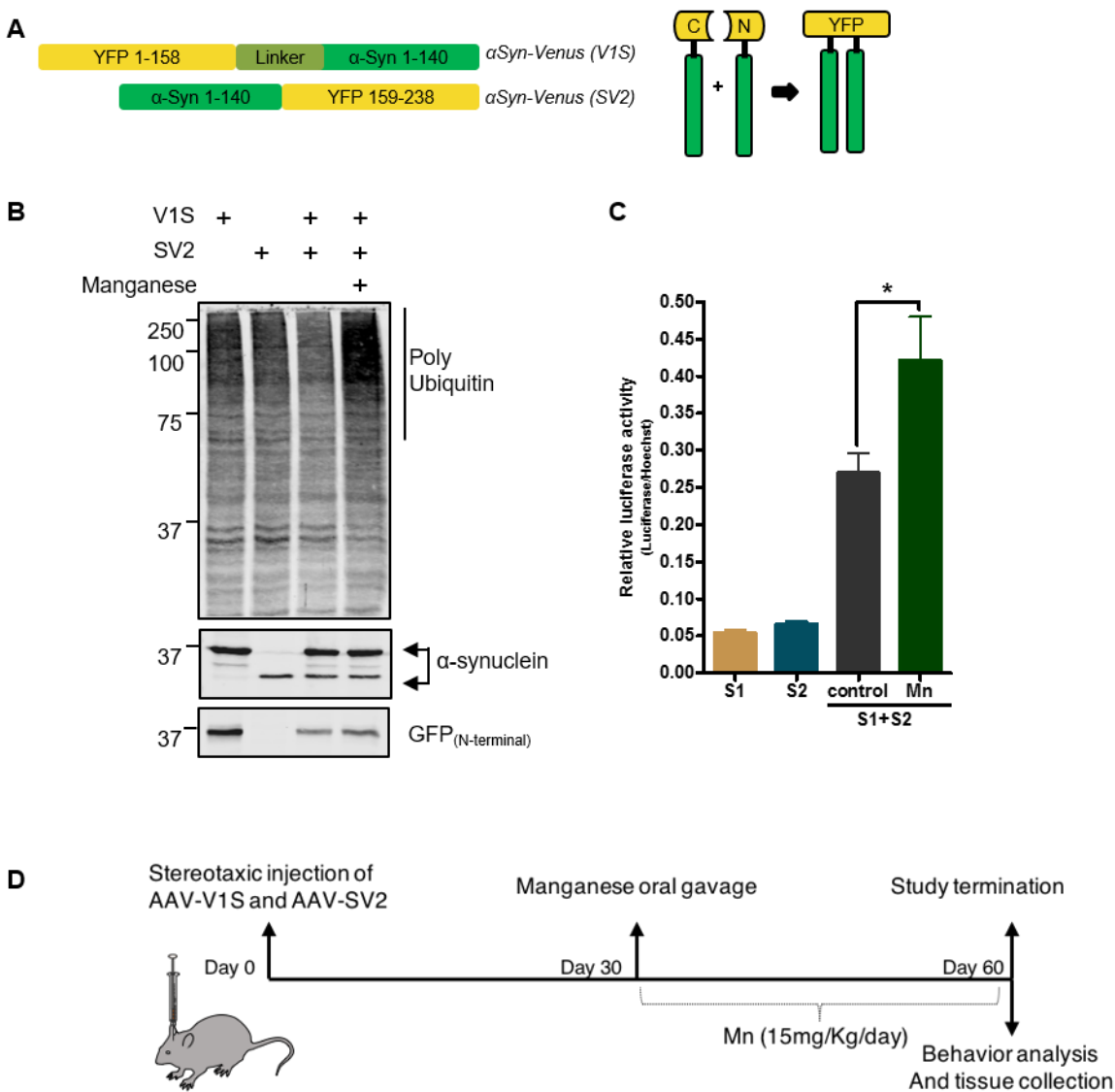


Figure S4: Visualization of cell-to-cell transmission of α Syn through protein fragment complementation assays. (A) Schematic representation of the BiFC constructs used for the assay. (B) Western blot of cells transfected with either S1V or SV2 and co-transfected with both constructs showing ubiquitin-immunopositive smears, which are indicative of a wide range of oligomeric species in Mn-treated cells. Immunoblots were also probed with an antibody against α Syn (middle) and GFP (bottom) to indicate effective transfection of BiFC constructs. Representative WBs of cell lysates from three individual experiments. (C) *Gaussia* luciferase protein fragment complementation assay with luciferase fused to α Syn molecules. Co-transfection of syn-hGLuc(1) and syn-hGLuc(2) results in a >5-fold increase in luciferase activity compared to background single transfections (syn-hGLuc(1) or syn-hGLuc(2)), indicative of at least a dimer formation. Mn-treated cells indicate further enhanced luciferase signal, indicative of more α Syn- α Syn interactions upon Mn exposure. Data are mean \pm SEM (* p <0.05) of three individual experiments performed in triplicate. (D) Schematic representation of study design for AAV8-BiFC and Mn exposure in WT mice.

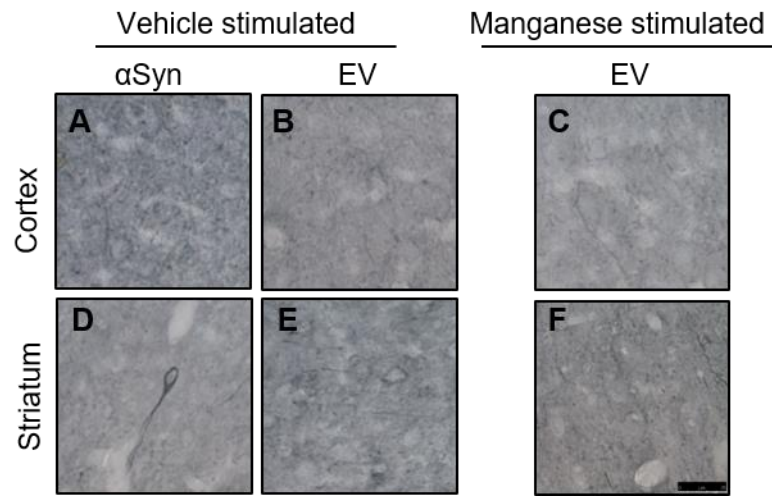


Figure S5: Vehicle-stimulated α Syn exosomes result in minimal α Syn pathology *in vivo*. (A to F) Images of p- α Syn pathology in mice injected with vehicle-stimulated α Syn exosomes (A: Cortex, D: Striatum). Images of p- α Syn pathology in mice receiving control vehicle-stimulated GFP exosomes (B and E) or Mn-stimulated GFP exosomes (C and F). Representative images from ≥ 12 animals per experimental group. Magnification, 60X. Scale bar, 25 μ m.